ATA Memo #36 - August 2001

Cancelling Satellite Interference at the Rapid Prototyping Array. A Comparison of Voltage and Power Domain Techniques.

D. A. Mitchell[1,2] and G. C. Bower[3]

1. School of Physics, The University of Sydney, Australia.
2. Australia Telescope National Facility, CSIRO, Australia.
3. Radio Astronomy Lab, University of California, Berkeley, USA.

Abstract

We present results of adaptive canceller experiments at the Rapid Prototyping Array which compare the quality of interference suppression achieved in the voltage and power domains. It is shown that if the optimal complex weights used to model the interference are stationary over the length of the time average, then the same level of suppression is achieved. A limitation of both methods is that the system noise in the reference voltage leads to an attenuation of the interference estimate. Using two reference signals with uncorrelated system noise improves the result, especially in the case where the reference signal has a low interference-to-noise ratio. For GLONASS and GPS interference on a baseline of a few tens of metres, it is shown that the complex weights are stable for several hundred milliseconds. A reduction of at least 36 dB of RFI power was achieved, this number limited by the amount of data available.

1 Introduction

In radio astronomy one is usually interested in the power distribution over the celestial sphere. Radio arrays generally combine the voltage output of many receivers in an attempt to measure this power. Techniques which remove unwanted power from this *output* have advantages over voltage techniques since they are applied to the integrated power, rather than the individual voltage samples[1]. On the other hand, if the individual voltages are needed (for example some of the SETI backends process the voltage streams rather than the power), these *power-domain* techniques will generally be inadequate.

This report attempts to make a quantitative comparison between two radio frequency interference (RFI) mitigation techniques applied to data collected at the *Rapid Prototyping Array* (RPA). In particular, voltage-domain techniques which are applied to the individual antenna voltages are compared with power-domain techniques which attempt to excise the RFI from the statistical correlations of antenna voltages. It has been conjectured that the level of RFI suppression achievable should be the same under certain conditions [1]. In section 2 an overview of the theory behind reference antenna based RFI cancellation using the Wiener solution is presented. This is followed in section 3 by some results of this theory applied to data containing satellite interference collected at the RPA.

Some of the factors that can affect RFI mitigation techniques include the length of time averages relative to the stationarity of the signal, (e.g. that of the transmitted signal itself, transmitter motion relative to delay-tracking centre, transmitter motion through antenna gain side lobes,

[1]Even though post correlation or post beamforming algorithms are applied less frequently, resulting in a smaller amount of processing, they need to be applied to each baseline or separate beam. Applying interference mitigation at an antenna level should become more efficient when the number of beams/baselines exceeds the number of antennas multiplied by the number of samples per integration.

stability of side lobes, multipath statistical stationarity, etc.), the effect of the number of bits at different stages of the receiver system, fractional-sample delay in XF correlators, and out of band RFI (ie. interference in the RF band before IF filtering). These issues need to be weighed up against the cost and complexity of both the front and back ends of a desired receiver system.

2 Reference Antenna Based RFI Cancellation Theory

In this section the voltage and correlation equations assumed for the RFI mitigation techniques are given. From these, reference antenna based RFI mitigation algorithms are derived. Unless otherwise stated, it is assumed that there is only one correlated interferer (that is, any correlation between the reference antenna signal and any of the primary antenna signals originates from a single source. Multipathing is neglected in this investigation). It is also assumed that any parameters used to model the interference are stationary on some time interval τ_{cs} (covariance stationary interval). Model parameters often come in the form of complex weights which affect the amplitude and phase of a reference signals spectrum so that it best matches that of the interference in any desired signal. They will usually change if an interfering satellite's position changes relative to either the pointing direction of the antennas (since the satellite moves through the antenna gain patterns), or the direction of the interferometers phase reference position (since the geometric delay of the signal will change).

The weights are usually calculated from either the lag or the frequency spectra of the signals. They are a function of the cross-correlation of the reference and primary signals, and are scaled in some way by the auto-correlation of the reference signal. This implies that if the relationship between the cross and auto correlations changes, then so will the weights. It also means that the statistics of the signal can change and not affect the weights so long as the overall effect on the relationship is zero. Care needs to be taken that the signals have not become decorrelated (due, for example, to bandwidth smearing or fringe-rotation decorrelation). Decorrelation often occurs when the stationarity assumptions have been broken. Throughout this report it is assumed that the interfering signal is in no way decorrelated and also that it is not strong enough to saturate any part of the system.

The IF voltage streams from the primary antennas (those pointing towards the astronomy field of interest) and the reference antenna/s (those pointing towards the interferer) consist of three components: A system noise voltage, n(t), a voltage due to all astronomical sources, s(t), and a voltage resulting from interference, i(t). It is assumed that n(t) is Gaussian, and that only one point source contributes to s(t) and one interferer to i(t). It is also assumed that all three voltage components are independent.

Consider a single reference antenna located at the reference position of the array. Let $\tau_s(t,k)$ and $\tau_i(t,k)$ represent the time delay between the reference antenna and the k^{th} primary antenna of the astronomy and RFI signals respectively. The voltage in the IF stream of a single polarisation of the k^{th} primary antenna is

$$v_{A_k}(t) = n_{A_k}(t) + g_{i,A_k}(t,\nu)i(t-\tau_{i,k}) + g_{s,A_k}(t,\nu)s(t-\tau_{s,k}),$$

where $n_{A_k}(t)$ is the system noise in the k^{th} antenna, g_{i,A_k} is the complex gain in the direction of the interferer for the k^{th} antenna, etc. The voltages in the two orthogonally polarised IF streams from the reference antenna are

$$\begin{aligned} v_{R_x}(t) &= n_{R_x}(t) + g_{i,R_x}(t,\nu)i(t) + g_{s,R_x}(t,\nu)s(t), \\ v_{R_y}(t) &= n_{R_y}(t) + g_{i,R_y}(t,\nu)i(t) + g_{s,R_y}(t,\nu)s(t), \end{aligned}$$

where the x and y subscripts denote the two orthogonal polarisations of the reference antenna, which are assumed to have independent system noise and be 100% polarised[2].

The integration and frequency intervals used are assumed to be narrow enough for the complex gains of the receiver systems, (g(t,ν) terms), to be essentially constant over the intervals. When the integrations become long enough for the stationary signal assumptions to fail, the quality of the RFI mitigation techniques will start to decline.

Transforming to the frequency domain, with subscript ν indicating a quasi-monochromatic frequency band centred at frequency ν, we have

$$\begin{array}{rcllll} v_{\nu_{A_k}}(t) & = & n_{\nu_{A_k}}(t) & + \; g_{\nu_{i,A_k}}(t)i_\nu(t)e^{j2\pi\nu\tau_{i,k}} & + & g_{\nu_{s,A_k}}(t)s_\nu(t)e^{j2\pi\nu\tau_{s,k}} \\ v_{\nu_{R_x}}(t) & = & n_{\nu_{R_x}}(t) & + \; g_{\nu_{i,R_x}}(t)i_\nu(t) & + & g_{\nu_{s,R_x}}(t)s_\nu(t) \\ v_{\nu_{R_y}}(t) & = & n_{\nu_{R_y}}(t) & + \; g_{\nu_{i,R_y}}(t)i_\nu(t) & + & g_{\nu_{s,R_y}}(t)s_\nu(t) \end{array} \quad (1)$$

For the rest of this document it is assumed that the gain of the reference antenna in the direction of the astronomy signal (ie. $g_{s,R}$) is zero. This will generally not be the case in reality, since a reference antenna will usually have some gain towards the sky, but for the purpose of this document the effect is assumed negligible. Any correlation of the astronomy signal between the reference and primary antennas will result in suppression of the astronomy signal.

2.1 Voltage-Domain RFI Cancellation

When using digital signal processing techniques in radio astronomy, care should be taken when naming processes and variables. Many communication reports talk about retrieving a desired signal from a noisy signal, and call the remaining signal the error. In radio astronomy RFI mitigation applications, the "desired" signal is usually the interference, and the "error" is actually desired. For this reason I will call the extracted signal the *interference* or *model* signal, and the signal remaining the *astronomy* or *residual* signal. Also, techniques which are applied to the voltages have been called "pre-correlation" methods while techniques applied to the statistics are often called "post-correlation" methods. The problem with this is that many voltage-domain techniques use the correlations in the RFI voltage modeling process, and therefore are also post-correlation techniques in a sense. For this reason they will be distinguished as *voltage* and *power* domain techniques. The standard derivations in this section can be found in many DSP texts, such as [6] and [4], and their applications in radio astronomy have been described in [3].

A standard method for predicting the properties of the interference in the astronomy antennas is to collect a copy of the interference that does not contain any of the astronomy information. This *reference* signal is used to form a model of the interference in the astronomy antenna signals. The model signal can be constructed by summing together many weighted versions of the reference signal. These weights are complex, containing a time delay and a scaling factor. The weights which reduce the power in the residual signal must also be the weights which reduce the interference, since it is the only correlated component of both voltage streams. In the frequency domain, this is equivalent to weighting and phase shifting each narrow sub-channel of the Fourier transformed reference voltage. This is easier to interpret, so the following equations all refer to operations on each narrow sub-channel of the frequency spectra, and all time integrations are carried out on

[2]The 100% polarised interference assumption might at times fail completely for the RPA with transmitters at the horizon. Many transmitters are linearly polarised, and since an X/Y mount has linearly polarised feeds rotating as a dish tracks around the horizon, there will be positions at which one of the feeds lines up with the transmitters polarisation. Both GLONASS and GPS satellites transmit circularly polarised signals and so the assumption should be alright for their interference.

each channel separately. See the appendix for the lag-domain version. The x polarisation of the residual voltage stream is given by

$$r_{\nu_{A_x}}(t) = v_{\nu_{A_x}}(t) - w_{\nu_{A_x,R_x}}(t) v_{\nu_{R_x}}(t), \tag{2}$$

where $w_{\nu_{A_x,R_x}}(t)$ is a vector containing the complex weights for each sub-channel. If the integrations are very long relative to the sample time (so that uncorrelated noise terms essentially drop to zero), but not long enough for the complex weight vector to change appreciably, then the power of the residual voltage is

$$< r^2_{\nu_{A_x}}(t) > \approx < v^2_{\nu_{A_x}}(t) > - w_{\nu_{A_x,R_x}} < v_{\nu_{A_x}}(t) v^*_{\nu_{R_x}}(t) > + w^2_{\nu_{A_x,R_x}} < v^2_{\nu_{R_x}}(t) > . \tag{3}$$

where the averaging "<>" is over time, τ_A, and frequency sub-channel $\Delta\nu$. In the complex weight domain $< r^2_{\nu_{A_x}}(t) >$ is a paraboloid with a definite minima. This minima must occur at the *optimal* weights which minimise the output power of equation 3. They are found by setting the derivative with respect to $w_{\nu_{A_x,R_x}}(t)$ to zero. Differentiating equation 3 gives the optimal weights for the x polarisation of astronomy antenna A at time t as

$$w_{\nu_{A_x,R_x}}(t) = \frac{< v_{\nu_{A_x}}(t) v^*_{\nu_{R_x}}(t) >}{< v^2_{\nu_{R_x}}(t) >}. \tag{4}$$

Applying these weights to the residual voltage from equation 2 gives

$$r_{\nu_{A_x}}(t) = v_{\nu_{A_x}}(t) - \frac{< v_{\nu_{A_x}}(t) v^*_{\nu_{R_x}}(t) >}{< v^2_{\nu_{R_x}}(t) >} v_{\nu_{R_x}}(t).$$

To investigate how well this cancellation should do, the residual power spectrum is estimated. From now, unless describing individual voltages, the explicit notation showing that a variable is time varying, *(t)*, will be dropped. In general if a quantity is inside angle brackets then it may be time varying. If the complex weights are constant over the integrations, which are long enough for the (independent, and therefore zero mean) system noise terms to have averaged very close to zero, then the power in the residual signal of antenna A is

$$\begin{aligned} R_\nu(A_k, A_k) &= < r_{\nu_{A_k}} r^*_{\nu_{A_k}} > \\ &\approx \left\langle \left(v_{\nu_{A_x}} - \frac{< v_{\nu_{A_x}} v^*_{\nu_{R_x}} >}{< v^2_{\nu_{R_x}} >} v_{\nu_{R_x}} \right) \left(v^*_{\nu_{A_x}} - \frac{< v^*_{\nu_{A_x}} v_{\nu_{R_x}} >}{< v^2_{\nu_{R_x}} >} v^*_{\nu_{R_x}} \right) \right\rangle \\ &\approx \left\langle v_{\nu_{A_x}} v^*_{\nu_{A_x}} \right\rangle - \frac{< v_{\nu_{A_x}} v^*_{\nu_{R_x}} >< v^*_{\nu_{A_x}} v_{\nu_{R_x}} >}{< v^2_{\nu_{R_x}} >}, \end{aligned} \tag{5}$$

where upper case characters represent the power of the lower case voltage variables. These expectation values are necessarily estimated by a finite number of samples, meaning that the noise is never completely averaged to zero. This will lead to injection of noise and an attenuation of the RFI power estimate. This limitation is discused in the next section. The striking thing about equation 5 is that if one is interested in power and is not concerned with the individual voltages, the RFI cancellation can be performed using these final statistical values [5]. These integrations may be over many thousands of samples, so applying the correction once at the end saves a lot of processing effort and time. To investigate the remaining RFI power, the voltage streams in equation 5 are broken in to their components

$$
\begin{aligned}
R_\nu(A_k,A_k) &\approx <n^2_{\nu_{A_k}}> + <g^2_{\nu_{s,A_k}}> S_\nu + <g^2_{\nu_{i,A_k}}> I_\nu - \\
&\quad \frac{<g_{\nu_{i,A_k}} g^*_{\nu_{i,R_x}}> I_\nu <g^*_{\nu_{i,A_k}} g_{\nu_{i,R_x}}> I_\nu}{<n^2_{\nu_{R_x}}> + <g^2_{\nu_{i,R_x}}> I_\nu} \\
&\approx <n^2_{\nu_{A_k}}> + <g^2_{\nu_{s,A_k}}> S_\nu + \\
&\quad \left(1 - \left(1 + \frac{<n^2_{\nu_{R_x}}>}{(<g^2_{\nu_{i,R_x}}> I_\nu)}\right)^{-1}\right) <g^2_{\nu_{i,A_k}}> I_\nu
\end{aligned} \tag{6}
$$

Equation 6 shows that even for the ideal case, where the weights are stationary and all of the uncorrelated noise is average out, not all of the RFI power is removed from the astronomy antenna power. A fraction related to the interference power to noise power ratio (INR) in the reference signal remains. The INR in the reference signal (INR_R) is defined as $\frac{(<g^2_{\nu_{i,R_x}}>I_\nu)}{<n^2_{\nu_{R_x}}>}$ and can be increased if a second reference antenna is used and two models are formed. The system noise terms in these models should be uncorrelated, and so average towards zero during the integration. The two reference signals used here are the two orthogonally polarised voltages from the reference antenna. This is convenient but not the only solution, and only applicable if the interfering signal is 100% polarised. When the two polarisations are not completely coherent, there will be an attenuation of the RFI power estimate. Also, there is usually cross-talk between the polarised feeds of antennas, so the cross-correlated system noise terms will not average towards zero. This is discussed in the next section. The system and interference are assumed ideal for the time being, so that the advantage of using two reference signals is obvious. Possible models for these dual-reference weights are given below and are indicated by $w'_{\nu_{A_x,R_x}}(t)$ and $w'_{\nu_{A_x,R_y}}(t)$.

$$
\begin{aligned}
w'_{\nu_{A_x,R_x}}(t) &= \frac{<v_{\nu_{A_x}}(t) v^*_{\nu_{R_x}}(t)>}{<v_{\nu_{R_x}}(t) v^*_{\nu_{R_y}}(t)>}, \\
w'_{\nu_{A_x,R_y}}(t) &= \frac{<v_{\nu_{A_x}}(t) v^*_{\nu_{R_y}}(t)>}{<v_{\nu_{R_x}}(t) v^*_{\nu_{R_y}}(t)>}.
\end{aligned} \tag{7}
$$

These weights are likely to be subset of the more general "multiple interferer" weights proposed by Geoffrey Bower [2]. It is shown in section 3 that the weights given in equation 7 do not remove interference to the same level as the dual reference signal power-domain method to be discussed shortly. It may be that there are terms missing from the weights given in equation 7. These weights are applied to the reference voltages in the following manner,

$$
\begin{aligned}
r'_{\nu_{x,A_x}}(t) &= v_{\nu_{A_x}}(t) - w'_{\nu_{A_x,R_x}}(t) v_{\nu_{R_y}}(t), \\
r'_{\nu_{y,A_x}}(t) &= v_{\nu_{A_x}}(t) - w'_{\nu_{A_x,R_y}}(t) v_{\nu_{R_x}}(t).
\end{aligned}
$$

The residual power spectrum of equation 6 is now estimated using the cross-correlation of these two residual voltages

$$
\begin{aligned}
R'_\nu(A_k,A_k) &= <r'_{\nu_{x,A_k}} r'^*_{\nu_{y,A_k}}> \\
&= <n^2_{\nu_{A_k}}> + <g^2_{\nu_{s,A_k}}> S_\nu + <g^2_{\nu_{i,A_k}}> I_\nu - \\
&\quad \frac{<g_{\nu_{i,A_k}} g^*_{\nu_{i,R_x}}> I_\nu <g^*_{\nu_{i,A_k}} g_{\nu_{i,R_y}}> I_\nu}{<g_{\nu_{i,R_x}} g^*_{\nu_{i,R_y}}> I_\nu} \\
&= <n^2_{\nu_{A_k}}> + <g^2_{\nu_{s,A_k}}> S_\nu.
\end{aligned} \tag{8}
$$

The difference between equations 5 and 8, resulting from the bandpass of the single reference signal in equation 5 is

$$
\Delta R_\nu(A_k,A_k) = <(g_{\nu_{i,A_k}} i_\nu(t))^2> (1 - \frac{1}{1 + 1/INR_R}). \tag{9}
$$

Similarly to the single reference antenna result from equation 6, if the integration time is short enough so that the optimal complex weights for the interference model remain stationary, all of the quantities can be estimated after correlation, and the power subtracted there.

2.2 Power-Domain RFI Cancellation

In section 2.1 it was shown that if the desired quantities of an observation are the power spectra, then the RFI suppression achieved by filtering individual voltages can be replicated after the power spectra are formed. This is only true for situations where the integration is taken over a time interval in which the optimal complex weights given by the Wiener solution remain constant. The main limitation in both cases is the interference-to-noise ratio in the reference signal, which results in a reduction in the amount of RFI subtracted. The situation can be improved by using a second reference (eg. two polarisations). In reality there is likely to be some correlation in the system noise of the two reference signals, which means that the interference-to-noise limitation is not removed, just made a lot better since the level of correlation will be much smaller. Another problem is noise added to what would be the perfect result due to finite sample integrations, finite FFTs, and other sampling effects. Some of these noise components are considered below.

Assuming that each temporal integration of length τ_A is in the regime where $\tau_A << \tau_{cs}$ and $\Delta\nu << \Delta\nu_{cs}$ (ie. there is insignificant decorrelation occurring over the times and frequency channels of interest), and using the geometric delay notation $\tau_{i,kl} = \tau_{i,k} - \tau_{i,l}$, the auto and cross-correlations of all antennas are formed

$$
\begin{aligned}
C_\nu(A_k, A_k, \tau_A) &= < v_{\nu_{A_k}} v^*_{\nu_{A_k}} > \\
&= < n^2_{\nu_{A_k}} > + < g^2_{\nu_{i,A_k}} > I_\nu + \\
&= < g^2_{\nu_{s,A_k}} > S_\nu + \mathcal{N}_{A_k,A_k}(\tau_A), \\
\\
C_\nu(A_k, A_l, \tau_A) &= < v_{\nu_{A_k}} v^*_{\nu_{A_l}} > \\
&= < g_{\nu_{i,A_k}} g^*_{\nu_{i,A_l}} e^{j2\pi\nu\tau_{i,kl}} > I_\nu + < g_{\nu_{s,A_k}} g^*_{\nu_{s,A_l}} e^{j2\pi\nu\tau_{s,kl}} > S_\nu + \\
&= \mathcal{N}_{A_k,A_l}(\tau_A), \\
\\
C_\nu(A_k, R_x, \tau_A) &= < v_{\nu_{A_k}} v^*_{\nu_{R_x}} > \\
&= < g_{\nu_{i,A_k}} g^*_{\nu_{i,R_x}} e^{j2\pi\nu\tau_{i,k}} > I_\nu + \mathcal{N}_{A_k,R_x}(\tau_A), \\
\\
C_\nu(R_x, R_x, \tau_A) &= < v_{\nu_{R_x}} v^*_{\nu_{R_x}} > \\
&= < n^2_{\nu_{R_x}} > + < g^2_{\nu_{i,R_x}} > I_\nu + \mathcal{N}_{R_x,R_x}(\tau_A), \\
\\
C_\nu(R_x, R_y, \tau_A) &= < v_{\nu_{R_x}} v^*_{\nu_{R_y}} > \\
&= < g_{\nu_{i,R_x}} g^*_{\nu_{i,R_y}} > I_\nu + \mathcal{N}_{R_x,R_y}(\tau_A).
\end{aligned}
\tag{10}
$$

The $\mathcal{N}(\tau_A)$ terms correspond to *uncorrelated* noise which is present in the correlations, but assumed to be thermal noise which will integrate to zero power as the integration time τ_A approaches infinity. There are many factors which can contribute to these terms, some of which, such as receiver cross-talk, may result in non-zero mean power. This needs to be looked into thoroughly, but for the time being is assumed to be mainly due to finite integrations of white thermal noise. The power-domain relations from section 2.1 can now be created from the correlations of equation 10. For a single reference signal the models are

$$
\begin{aligned}
M_\nu(A_k, A_k, \tau_A) &= \frac{C_\nu(A_k,R_x)C^*_\nu(A_k,R_x)}{C^*_\nu(R_x,R_x)} \\
&= \frac{<g^2_{\nu_{i,A_k}}>I_\nu}{1+INR_R^{-1}+\frac{\mathcal{N}_{R_x,R_x}(\tau_A)}{<g^2_{\nu_{i,R_x}}>I_\nu}} + \mathcal{N}'_{A_k,A_k}(\tau_A) \\
M_\nu(A_k, A_l, \tau_A) &= \frac{C_\nu(A_k,R_x)C^*_\nu(A_l,R_x)}{C^*_\nu(R_x,R_x)} \\
&= \frac{<g_{\nu_{i,A_k}} g^*_{\nu_{i,A_l}} e^{j2\pi\nu\tau_{i,kl}}>I_\nu}{1+INR_R^{-1}+\frac{\mathcal{N}_{R_x,R_x}(\tau_A)}{<g^2_{\nu_{i,R_x}}>I_\nu}} + \mathcal{N}'_{A_k,A_l}(\tau_A)
\end{aligned} \tag{11}
$$

where $INR_R = \frac{<g_{\nu_{i,A_k}} g^*_{\nu_{i,A_l}}>I_\nu}{<n^2_{\nu_{R_x}}>}$, and the higher order uncorrelated noise components generated in the above multiplications are represented by the $\mathcal{N}'(\tau_A)$ terms.

For the two reference signal case, where the two orthogonally polarised reference receiver outputs are used as the two reference signals, equation 11 becomes

$$
\begin{aligned}
M_\nu(A_k, A_k, \tau_A) &= \frac{C_\nu(A_k,R_x)C^*_\nu(A_k,R_y)}{C^*_\nu(R_x,R_y)} \\
&= \frac{<g^2_{\nu_{i,A_k}}>I_\nu}{1+\frac{<n^*_{\nu_{R_x}} n_{\nu_{R_y}}>}{<g^*_{\nu_{i,R_x}} g_{\nu_{i,R_y}}>I_\nu}+\frac{\mathcal{N}_{R_x,R_y}(\tau_A)}{<g^*_{\nu_{i,R_x}} g_{\nu_{i,R_y}}>I_\nu}} + \mathcal{N}'_{A_k,A_k}(\tau_A) \\
M_\nu(A_k, A_l, \tau_A) &= \frac{C_\nu(A_k,R_x)C^*_\nu(A_l,R_y)}{C^*_\nu(R_x,R_y)} \\
&= \frac{<g_{\nu_{i,A_k}} g^*_{\nu_{i,A_l}} e^{j2\pi\nu\tau_{i,kl}}>I_\nu}{1+\frac{<n^*_{\nu_{R_x}} n_{\nu_{R_y}}>}{<g^*_{\nu_{i,R_x}} g_{\nu_{i,R_y}}>I_\nu}+\frac{\mathcal{N}_{R_x,R_y}(\tau_A)}{<g^*_{\nu_{i,R_x}} g_{\nu_{i,R_y}}>I_\nu}} + \mathcal{N}'_{A_k,A_l}(\tau_A)
\end{aligned} \tag{12}
$$

The denominators of equation 12 approach unity as the integration time approaches infinity and the receiver independence improves. As these noise terms move closer to zero, and when the interference-to-noise ratio is low, using two reference signals in either the voltage or power domain gives a vast improvement in RFI reduction and noise injection compared with a single reference signals, as long as the interference in the two reference signals is coherent.

3 Results

Most of the theoretical results from section 2 have been tested on data taken at the RPA while pointing toward GLONASS, GPS, and IRIDIUM satellites. These tests and their results are described in this section.

Unless otherwise stated, each observation and analysis underwent the following steps. A total of 2.23 seconds of dual polarised voltage data was recorded at a rate of 30 MSamples per second with 8 bit sampling for each RPA antenna. This is equivalent to 255*256*1024 samples per voltage stream. Each consecutive set of 1024 samples was transformed into the frequency domain, resulting in 255*256 spectra containing 512 frequency channels, each $\sim$ 30 kHz wide. For each of these frequency channels, 255 consecutive correlations were formed from 256 samples. At the end of each correlation *block*, ($\sim$ 8.74 ms), the new correlations were used to estimate the RFI power in the primary antennas power spectra, and also to generate new weights for the next 8.74 ms of voltage-domain RFI cancellations. All raw and clean power spectra were averaged over the

255 blocks to give the results shown. This indicates a major difference between the voltage and power domain results. The voltage-domain subtractions used the *previous* block to estimate the RFI voltages, while the power-domain subtractions used the *current* block to estimate the RFI power. In the ATA there may be a built-in voltage delay, meaning that the weights from the *current* block can be used on the voltages that generated them. This delay should be included in future comparisons. It should also be noted that the voltage domain subtractions were applied in the time domain, that is, using lag spectra and delayed voltages for the modeling.

3.1 GLObal NAvigation Satellite System (GLONASS) Satellite 779

In this section results from an observation of a GLONASS satellite are presented. The observation consisted of recording 2.23 seconds of dual polarised voltage data, with 8 bit sampling at a rate of 30 MSamples per second. Data was taken while pointing toward the satellite GLONASS 779 (COSMOS 2364). GLONASS 779 transmits a 1.0 MHz phase modulated coarse acquisition (C/A) signal with a chip rate of 0.511 Mbits per second, and a 10.0 MHz phase modulated precise (P) signal with a chip rate of 5.11 Mbits per second. The C/A signal power is $\approx$ 10 dB greater than the P signal power, and is the obvious central peak in the following figures. Both signals are centred at 1603.1250 MHz. The observation was run on June 21, 2001, at approximately 18:47 UT, and was centred at 1603 MHz. Antenna 1 was pointing toward the satellite with an azimuth of 344° and an elevation of 68°. For this experiment antennas 3 and 4 were used as the astronomy antennas. Antenna 3 was given an azimuth offset of $+4^o$ while antenna 4 was given an azimuth offset of +8°. These offsets were made to ensure some variation in the interference-to-noise ratios of the astronomy antennas. In all figures, dashed lines indicate bandpass estimates. A fifth order polynomial fit of the dual reference power-domain cleaned spectra were generally used for these estimates. In some cases this fit is obviously inaccurate, and the bandpass shapes are currently being modeled.

Figure 1 shows the auto-correlation power spectra for each of the antennas. 8.74 ms integrations were averaged together to give the power over the 2.23 second observation. In this figure the two columns are equivalent, just shown on different scales. Antenna 3 has similar RFI power levels to the reference (antenna 1), while the RFI power in antenna 4 is an order of magnitude weaker.

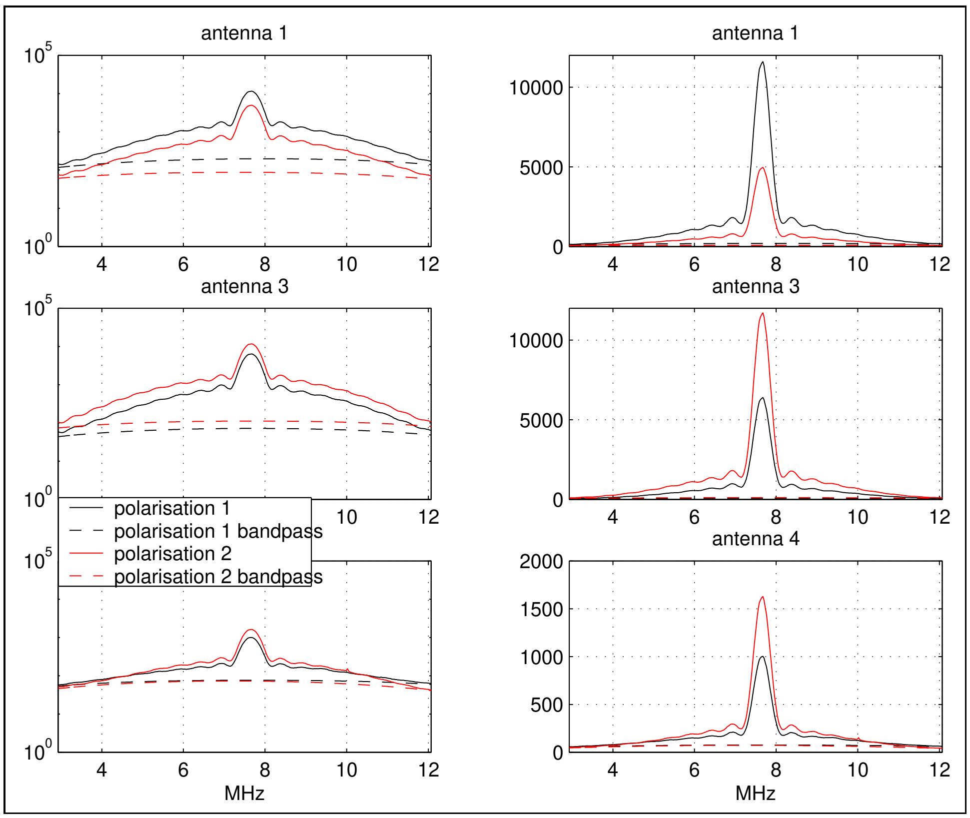

Figure 1: *Observed power in antennas 1, 3, and 4. Antenna 1 was pointing at GLONASS 779, while antennas 3 and 4 were offset in azimuth by +4 and +8 degrees respectively. The power was estimated by correlating the output of 256 1024-pt FFTs (8.74 ms) and averaging the results over 2.23 seconds. Red and black lines distinguish the two receiver polarisations, with dashed lines indicating bandpass estimates. The left and right columns are equivalent, apart from log and linear vertical scales.*

Figure 2 shows the results of different RFI mitigation techniques for the two astronomy antennas (3 and 4). Each antenna is shown in a separate row, and each polarisation in a separate column. The dual reference voltage-domain residuals (magenta lines) were only calculated for antenna 4. This is due to the fact that using the two reference antenna polarisations gave extremely noisy data, and needs more investigation, so the same polarisation of antenna 3 was used as the second reference. All of the dual reference residuals have a lower power than the the single reference residuals. This is mainly due to the additional INR_R term in the denominator of equation 6 and shown in more detail in figure 3.

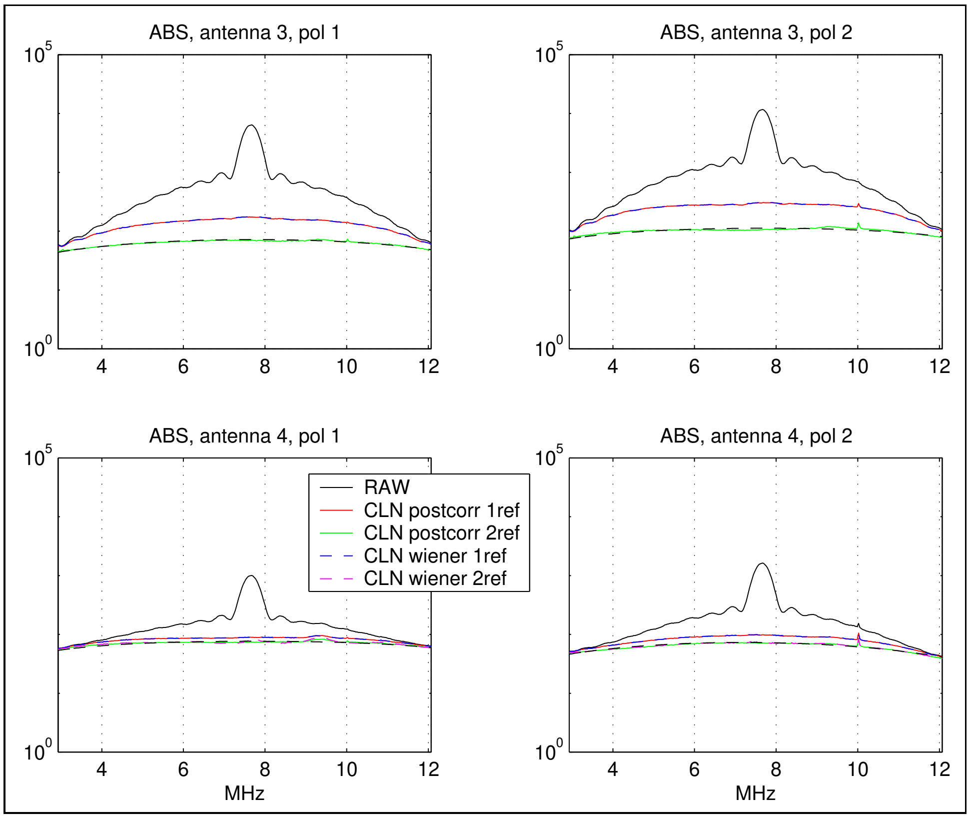

Figure 2: *Residuals of various RFI mitigation techniques applied to the GLONASS 772 data. In each of the four sub-plots, black lines indicate raw power, (see figure 1). The middle set of lines in each sub-plot show the residuals of techniques which used a single polarisation of antenna 1 only. In the lower set of lines, dashed black lines indicate bandpass estimates, while green lines represent power domain cancellation using both polarisations from antenna 1 to estimate the RFI power. Magenta lines in the bottom plots (antenna 4) represent dual reference voltage-domain cancellation, with single polarisations from antennas 1 and 3 being used as the reference signals. See figure 3 for a zoomed view of antenna 4. Using two reference signals removes more of the RFI power, due mainly to the independence of the reference antenna system noise terms, (see equation 12).*

Figure 3 shows a zoomed view of the GLONASS residuals of antenna 4. The peak at 9.3 MHz is due to a second GLONASS transmission (see figure caption), while the peak at 10 MHz is a birdie of the receiver system. The bandpass estimates (dashed black lines) have been estimated from a fit of the dual reference power-domain spectra (green lines). While this is not the best fit, spectra collected after this observation, when the satellite had moved away, confirmed that these are close to the actual bandpasses. The error occurring around the C/A 1 MHz peak for the dual reference voltage-domain spectra (magenta lines) is currently unaccounted for. This will be analysed in the near future.

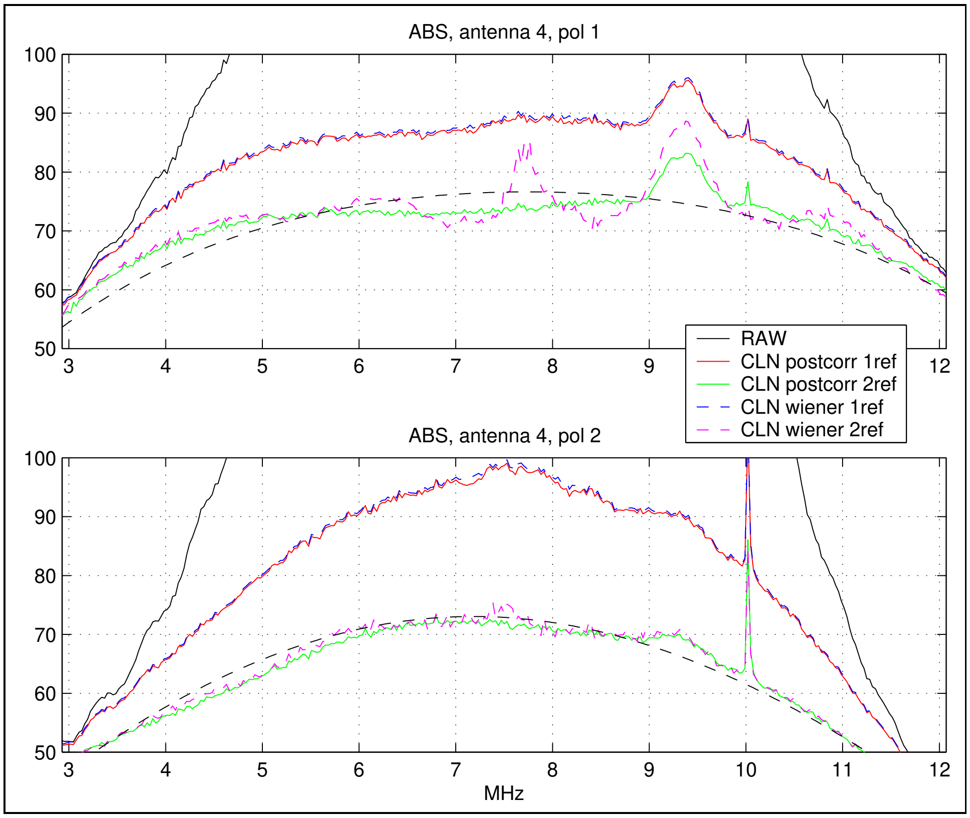

Figure 3: *Zoomed version of the RFI residuals in the power spectra of antenna 4 (bottom plots in figure 2). Shown are the results of four RFI mitigation techniques used to remove the GLONASS RFI. The peak at $\approx$ 9.3 MHz is attributed to a second satellite. At the time of observation, GLONASS 787 (COSMOS 2375) which transmits approximately 1.7 MHz above GLONASS 779 at 1604.8125 MHz was above the horizon. This places its central frequency at baseband at 9.31 MHz. This is consistent with the secondary peak. Its position at the time was azimuth* = 248° *and elevation* = 82°. *Note that using 2 reference signals in the voltage domain does a good job for the P signal, but fails slightly for the strong C/A signal. This has not been investigated.*

The fraction of RFI power remaining in the single reference residuals is largely due to the bandpass of the reference signal, and is a function of the reference signal interference-to-noise ratio. If it is assumed that the dual reference residuals contain a relatively small amount of RFI residual, then the difference between the single and dual residual power gives an estimate of the RFI power remain in the single reference residuals. This quantity is summarised in equation 9. Figure 4 shows the predicted result from equation 9 (black lines), together with the measured differences made using the bandpass estimates shown in figure 1. The deviation of the dual reference voltage-domain residuals and the dual reference power domain-residuals is also shown (magenta). These results (which assume the only error to be the reference bandpasses) seem to indicate that this correlated system noise is a major limitation to the single reference signal techniques (relative to the dual reference techniques).

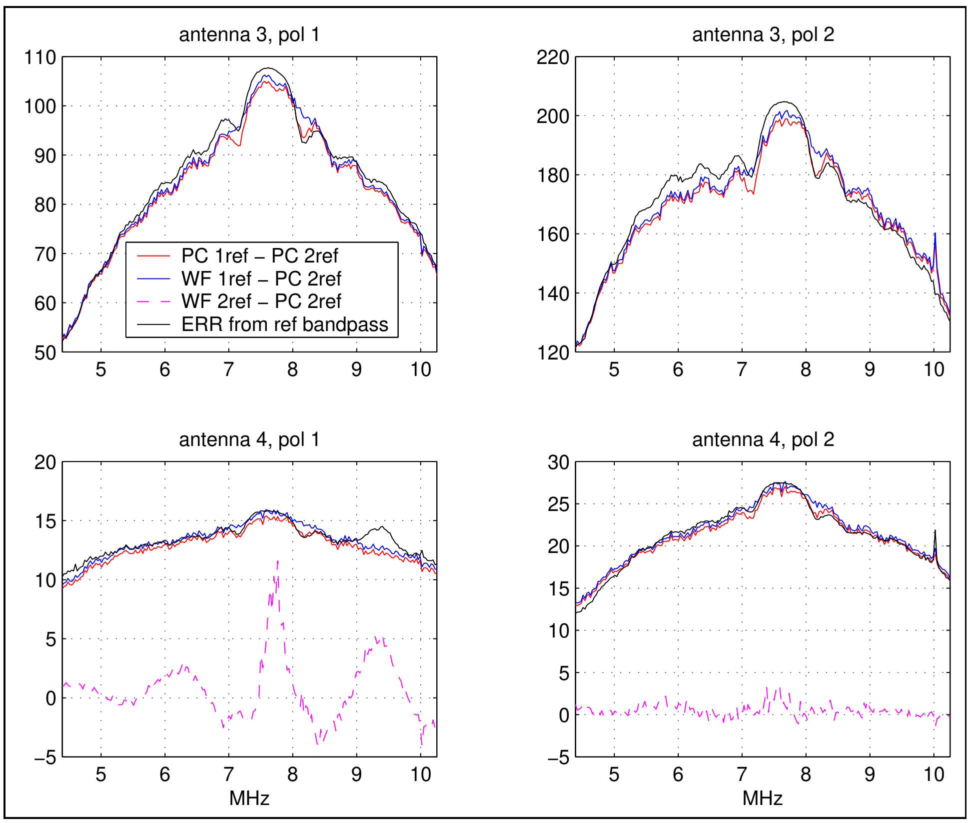

Figure 4: *Observed and estimated RFI residual power for each mitigation result apart from the dual reference power domain method. The dual reference power domain method, fitted with a 5^{th} order polynomial, was used as a bandpass estimate. The main reason for the RFI residual power in the single reference residuals is the reference antenna bandpass. The theoretical difference due to the system noise is given by equation 9* $\left(< (g_{\nu_{i,A_k}} i_\nu(t))^2 > (1 - \frac{1}{1+1/INR_R})\right)$, *and is indicated by black lines.*

Figure 5 shows the increased error when the single reference voltage-domain weights are calculated from a single FIR filter (from the first 1024-pt FFT for each sub-correlation block). This is attributed to the zero mean noise terms in the weight estimates ($\mathcal{N}(\tau_A)$ terms given in section 2.2) still being significant due to an insufficient number of samples in the estimate.

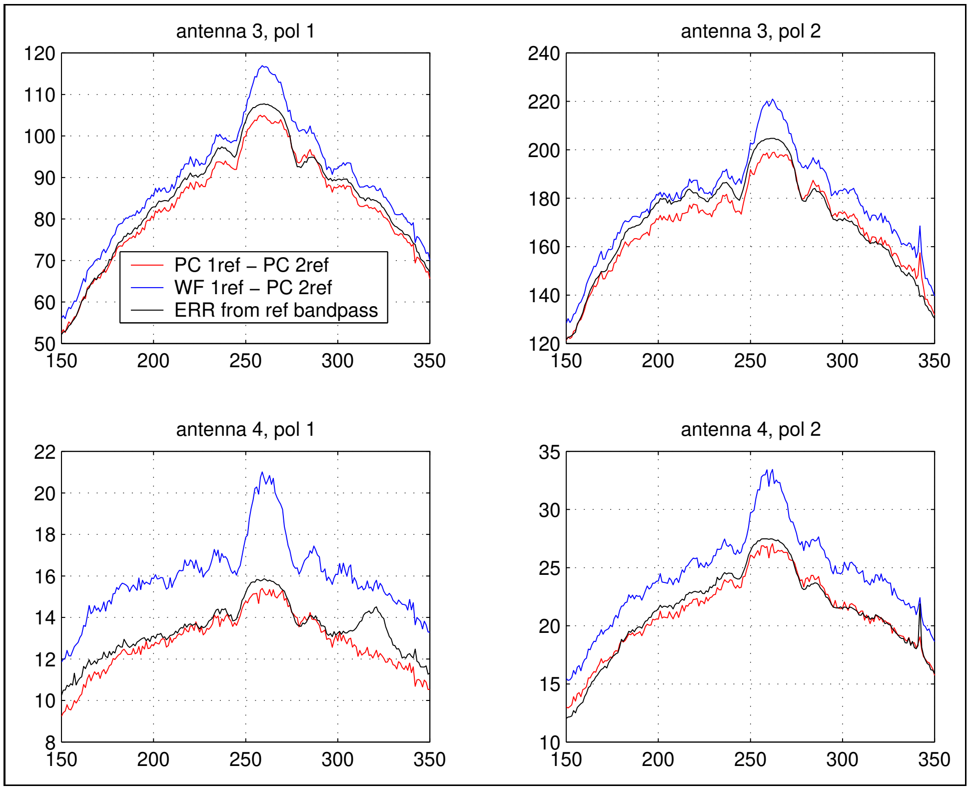

Figure 5: *Observed and estimated RFI residual power for each mitigation result apart from the dual reference power domain method. The FIR filter weights used in the single reference voltage domain method (blue lines) were calculated from the first 1024 samples in each 8.74 ms integration. This results in noisy weights, leading to extra noise in the residuals.*

Figure 6 shows the RMS in the C/A peak of each residual power spectra divided by the RMS in the C/A peak of the raw power spectra, as a function of integration time. Points represent the ratio measured at the end of each 8.74 ms integration. Curves following a $t^{-1/2}$ trend indicate thermal noise domination, where the noise in the residual power spectra is decreasing as $\sqrt{2\tau\Delta\nu}$. When the structured RFI remnants start to dominate, the power ratio should converge to a constant value. It is important that the signal is structured in the region that the RMS is estimated. The mean power across the spectrum is subtracted out during the RMS estimate, so a flat signal will not affect the RMS. The RMS values can not in general be used in INR estimates, but should be an adequate estimate of INR reduction (if the signal is not flat).

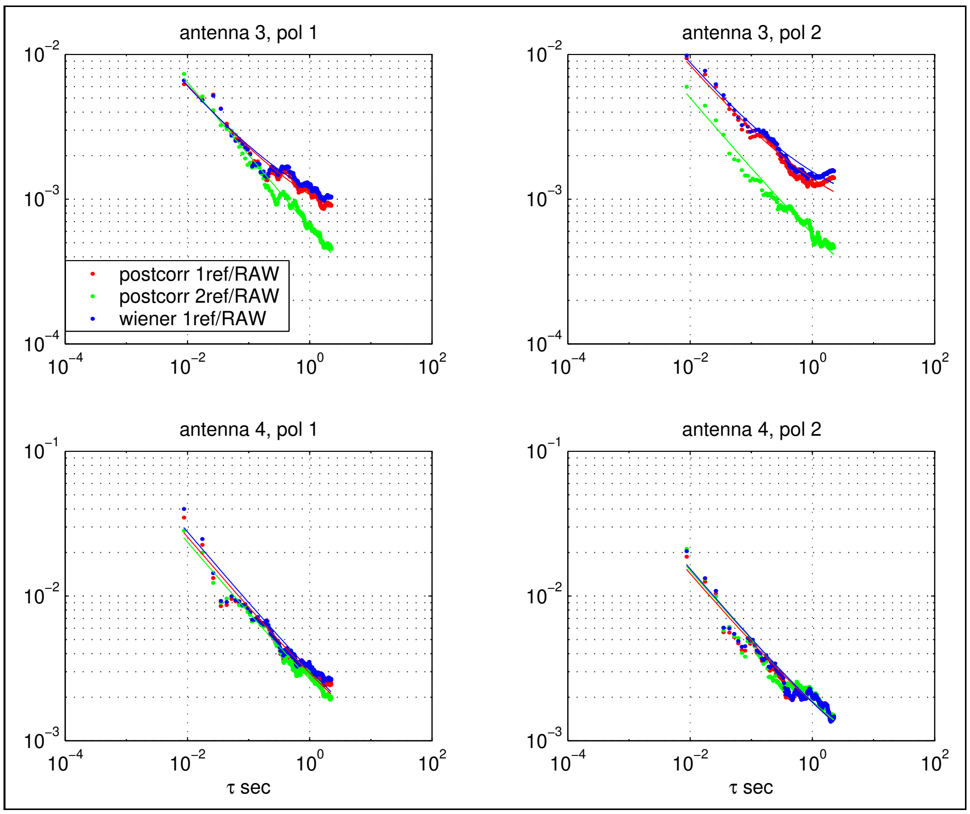

Figure 6: *RMS in the residual power divided by the RMS in the raw power over the 1 MHz GLONASS C/A peak. Smooth lines indicate the best fit for* $P = A + Bt^{-1/2}$*, where P is the power and A and B are constants. If the raw data RMS is dominated by a structured signal, and the residual RMS is dominated by thermal noise then this ratio should decrease as* $t^{-1/2}$*. When the residual RMS becomes dominated by the structured signal the ratio should start to converge. It is shown that approximately 36 dB of RFI power reduction has been achieved, and that the reduction has not reached it limit after 2.23 seconds, except for the second polarisation of antennas 3.*

To investigate the stability of the voltage domain weights, one set of weights were calculated from the first 8.74 ms correlation, and used for the entire 2.23 seconds. Figure 7 shows the effect on the residual/raw power spectra RMS ratios (compare with figure 6). Note that the weights were only held constant for the voltage domain weights. The power domain weights were adapted as before. When the weights are no longer appropriate the interference power in the residuals should start to increase, as it does in the figure. These results show that an update time of a few hundred milliseconds is adequate for the GLONASS interference (although a detailed analysis of this is currently underway). This is a lot longer than the chip rate of the C/A signal (0.511 MHz phase modulation $\approx$ 2 milliseconds). The reason for this is that if the transmitted signals statistics change, but the band *shape* stays constant, the complex weights should stay the same. The weight estimate is made on each sub-frequency channel separately, so as long as the ratio of the RFI power in the reference signal to that in the primary signal stays constant, and the geometric delay stays the same, so should the weights. If the transmission doesn't move out of any current frequency channels (or in to new ones), then the main effect on the weights will be due to satellite motion. This causes a change in relative power in the primary and reference antennas (due to motion through the antenna side lobes), and a change in the geometric delay of the RFI signal.

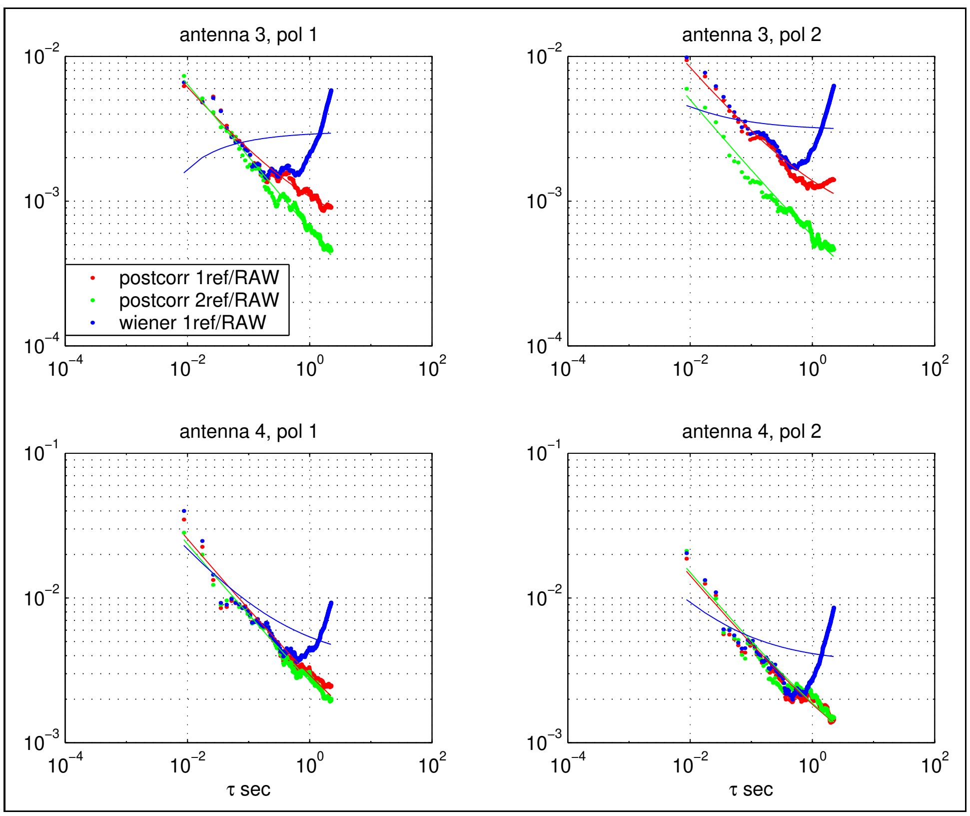

Figure 7: *RMS in the residual power divided by the RMS in the raw power over the 1 MHz GLONASS C/A peak. Smooth lines indicate the best fit for* $P = A + Bt^{-1/2}$*, where* P *is the power and* A *and* B *are constants. If the raw data RMS is dominated by a structured signal, and the residual RMS is dominated by thermal noise then this ratio should decrease as* $t^{-1/2}$*. When the residual RMS becomes dominated by the structured signal the ratio should start to converge. If the structured signal in the residual starts to grow, then so will this RMS ratio. The rise in the blue lines, representing the static weights, indicates that after several hundred msecs the weights are no longer appropriate. This could be due to a change in the transmitter relative to the antenna gain patterns, or the interferometer delay pattern, or it may be due to other effects. This needs to be investigated more thoroughly.*

Since the limit of the techniques were not reached after 2.23 seconds, another observation was carried out with nine 2.23 second acquisitions, taken approximately 2 minutes apart. New weights were calculated at the beginning of each acquisition, so the change in satellite location should have a minimal effect (the main due to changes in the received transmitter power, meaning changes in the RMS ratios may be due to the raw power rather than just the residual power). Nevertheless, the RFI power reduction is seen to still be effective after many seconds, and some of the deviation from $t^{-1/2}$ may be attributable to a secondary GLONASS satellite. Figure 8 shows the RMS ratio over 20.07 seconds of integration for the RFI mitigation techniques. The observation is of GLONASS 788, which transmits C/A and P signals centred at 1603.688 MHz. GLONASS 785 transmits at 1604.250 MHz and may be responsible for some of the deviation. All of the astronomy antennas were pointing at an OH maser source (OH26.5), and the reference antenna (antenna 2) was tracking the satellite. The satellite came closest to the OH maser at about 9 seconds into the 20 seconds of data, and the variation in the RMS is likely to be related to this change in RFI power in the astronomy antenna. More work needs to be done on the individual 2.23 seconds data to find correlations in amplitude deviations.

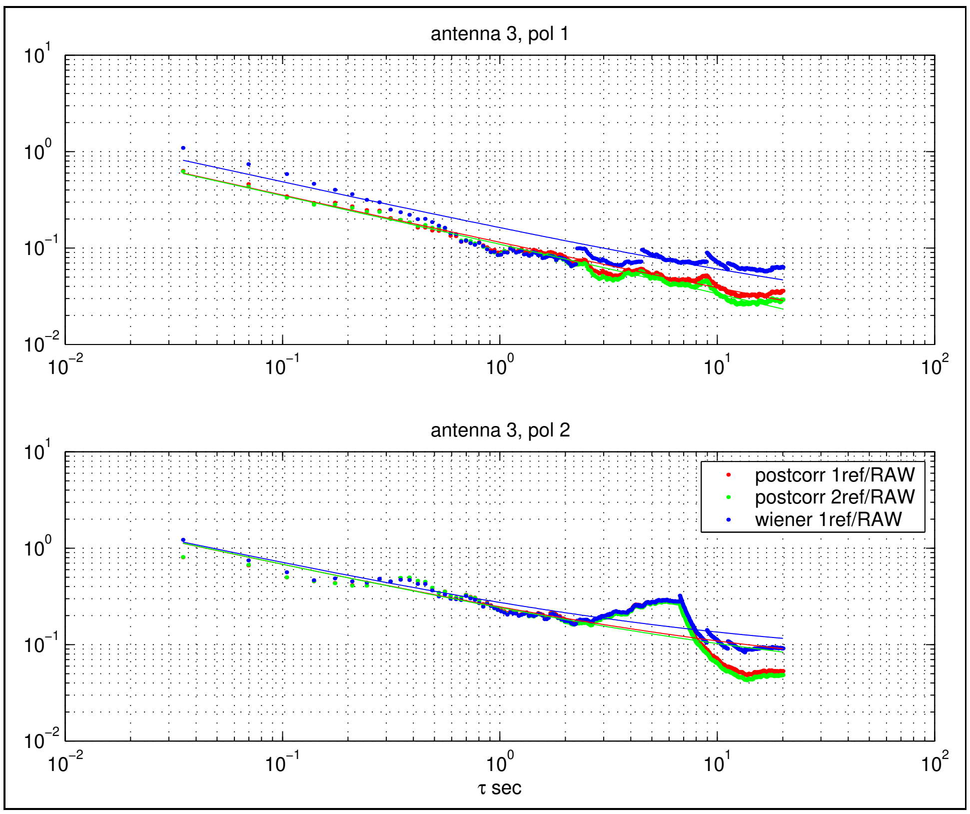

Figure 8: *RMS in the residual power divided by the RMS in the raw power over the 1 MHz GLONASS C/A peak. Smooth lines indicate the best fit for $P = A + Bt^{-1/2}$, where P is the power and A and B are constants. If the raw data RMS is dominated by a structured signal, and the residual RMS is dominated by thermal noise then this ratio should decrease as $t^{-1/2}$. When the residual RMS becomes dominated by the structured signal the ratio should start to converge. It is shown that the reduction may have reached it limit between 10 and 20 seconds, but further investigation is needed.*

3.2 Global Positioning System (GPS) Satellites

In this section results from an observation of a GPS satellite are presented. The observation consisted of recording 2.23 seconds of dual polarised voltage data, with 8 bit sampling at a rate of 30 MSamples per second. Data was taken while pointing toward the satellite GPS BIIA-17 (PRN 29). GPS BIIA-17 transmits a 2.046 MHz phase modulated coarse acquisition (C/A) signal with a chip rate of 1.023 Mbits per second, and a 20.46 MHz phase modulated precise (P) signal with a chip rate of 10.23 Mbits per second. The C/A signal power is $\approx$ 10 dB greater than the P signal power, and is the obvious central peak in the following figures. Both signals are centred at 1575.42 MHz. The observation was run on June 19, 2001, at approximately 17:44 UT, and was centred at 1575.42 MHz. Antenna 1 was pointing toward the satellites direction with an azimuth of 42° and an elevation of 53°. In these results antennas 3 and 4 were used as the astronomy antennas. Antenna 3 was given an azimuth offset of +3° while antenna 4 was given an azimuth offset of +6°. These offsets were made to ensure that the INR in the primary astronomy antennas was not equal for all receivers. Figure 9 shows the auto-correlation power spectra for each of the antennas. 8.74 ms integrations were averaged together to give the power over the 2.23 second observation. In this figure the two columns are equivalent, just shown on different scales. Antenna 3 has similar RFI power levels to antenna 1, but the RFI power in antenna 4 is an order of magnitude weaker.

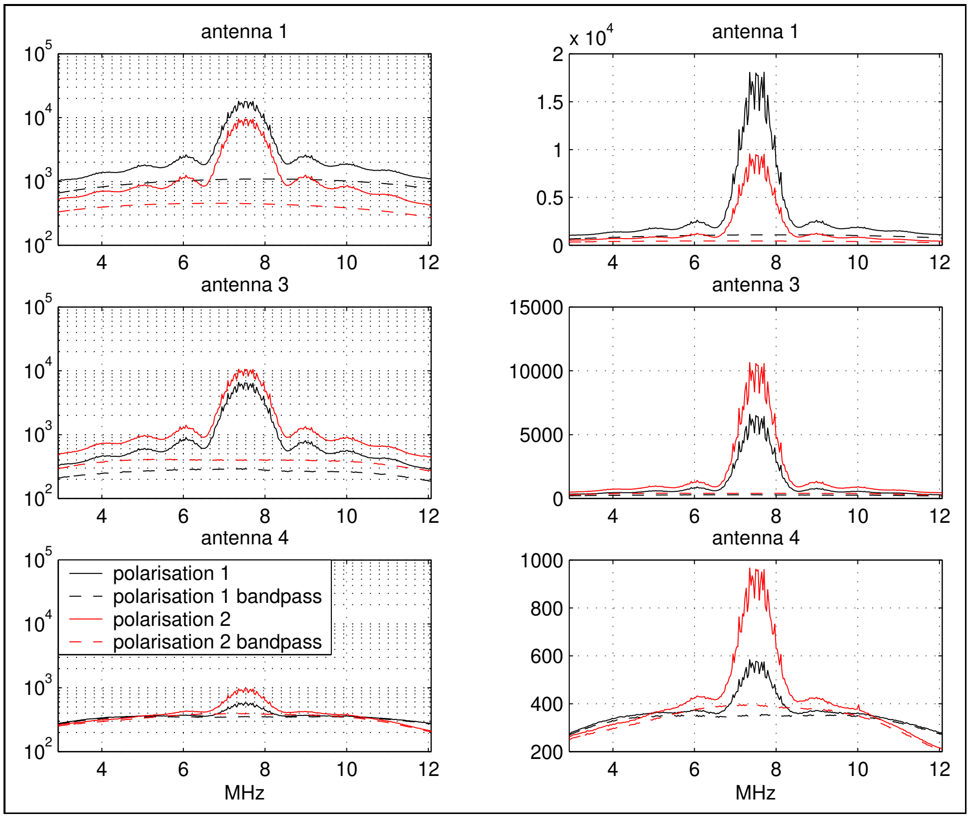

Figure 9: *Observed power in antennas 1, 3, and 4. Antenna 1 was pointing at GPS BIIA-17, while antennas 3 and 4 were offset in azimuth by +3 and +6 degrees respectively. The power was estimated by correlating the output of 256 1024-pt FFTs (8.74 ms) and averaging the results over 2.23 seconds. Red and black lines distinguish receiver polarisations, with dashed lines indicating bandpass estimates. The left and right columns are equivalent, apart from log and linear vertical scales.*

Figure 10 shows the results of different RFI mitigation techniques for the two astronomy antennas (3 and 4). Each antenna is shown in a separate row, and each polarisation in a separate column. The dual reference voltage-domain residuals (magenta lines) were only calculated for antenna 4. They were calculated using a single polarisation of from antennas 1 and 3 as references. All of the dual reference residuals have a lower power than the the single reference residuals. This is mainly due to the additional INR_R term in the denominator of equation 6 and shown in more detail in figure 11.

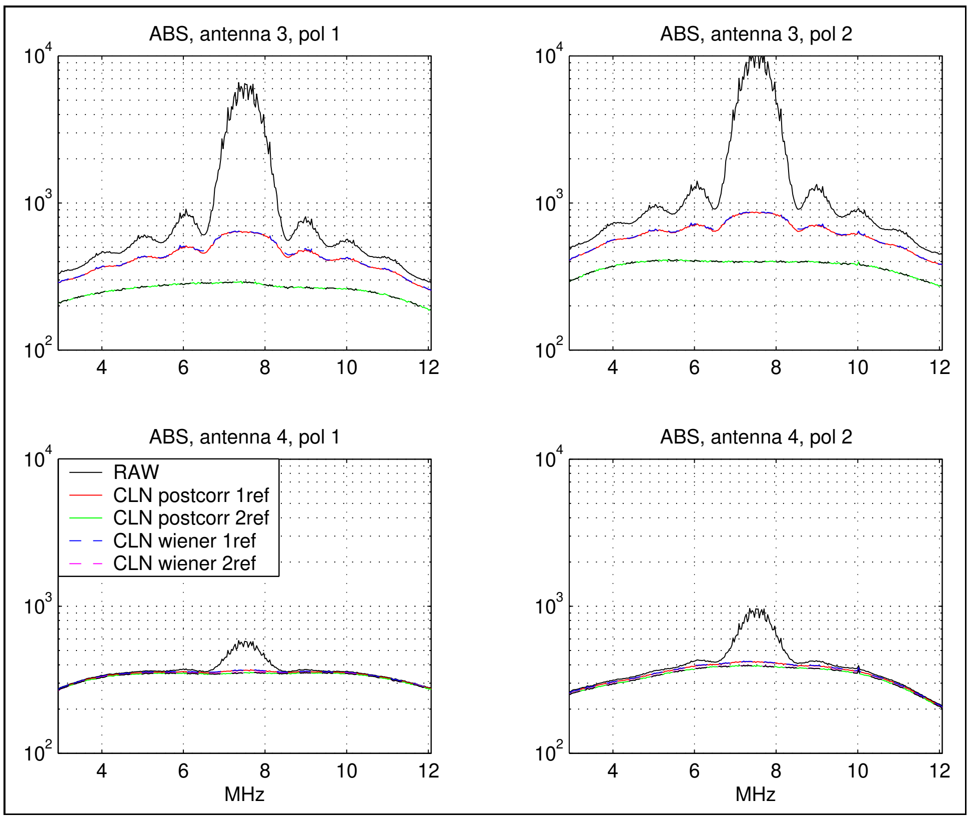

Figure 10: *Residuals of various RFI mitigation techniques applied to the GPS BIIA-17 data. In each of the four sub-plots, black lines indicate raw power, (see figure 9). The middle set of lines in each sub-plot show the residuals of techniques which used a single polarisation of antenna 1 only. In the lower set of lines, dashed black lines indicate bandpass estimates, while green lines represent power-domain cancellation using both polarisations from antenna 1 to estimate the RFI power. Magenta lines in the bottom plots (antenna 4) represent dual reference voltage-domain cancellation, with single polarisations from antennas 1 and 3 being used as the reference signals. See figure 11 for a zoomed view of antenna 4. Using two reference signals removes more of the RFI power, due mainly to the independence of the reference antenna system noise terms, (see equation 12).*

Figure 11 shows a zoomed view of the GPS residuals of antenna 4. The peak at 10 MHz is a birdie of the receiver system. Some of the reamining power in all of the residuals may be due to additional satellites, however this is harder to test since all GPS satellites transmit at the same frequency. Lag and Doppler information should provide some indication of how much power is expected from all other satellites above the horizon. This is left to future work.

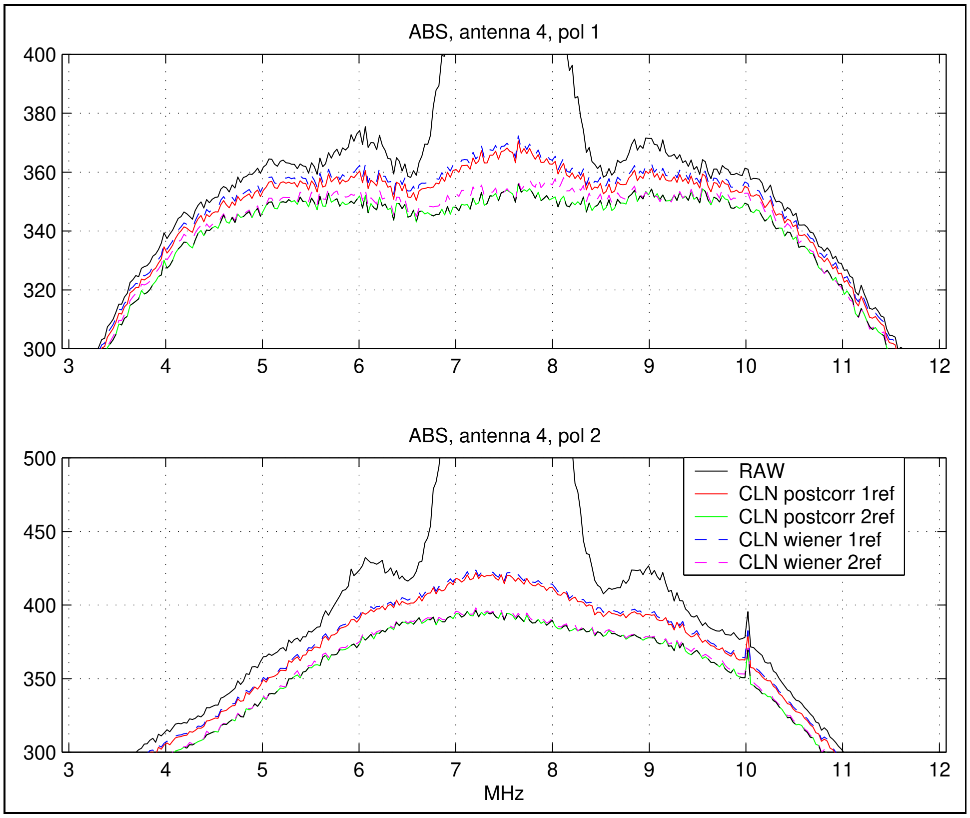

Figure 11: *Zoomed view of the GPS residuals of antenna 4 (see figure 10). The peak at 10 MHz is a birdie of the receiver system. It is not clear at the moment how much of the residual power is due to other satellites which were in transit at the time of observation. Lag and Doppler information will help in this investigation.*

Figure 12 shows the RMS in the C/A peak for each residual power spectra divided by the RMS in the C/A peak for the raw power spectra as a function of integration time. These results are similar to those of GLONASS (figure 6) which has a similar orbital period.

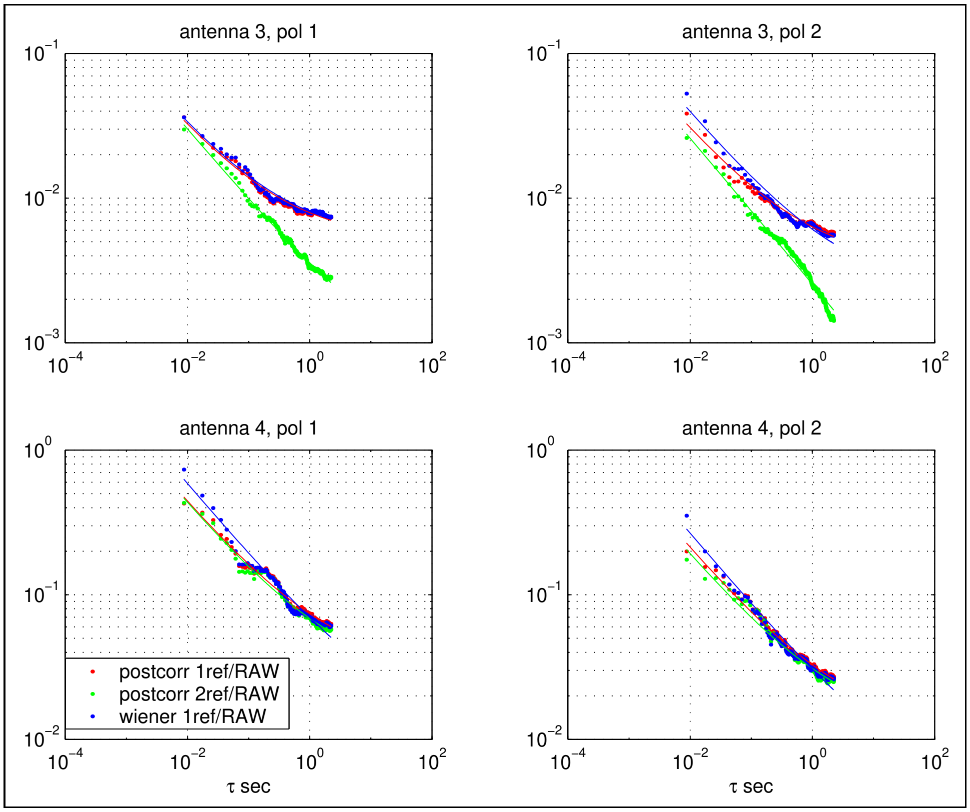

Figure 12: *RMS in the residual power divided by the RMS in the raw power over the 2 MHz GPS C/A peak at the centre of the band. Smooth lines indicate the best fit for $P = A + Bt^{-1/2}$, where P is the power and A and B are constants. If the raw data RMS is dominated by a structured signal, and the residual RMS is dominated by thermal noise then this ratio should decrease as $t^{-1/2}$. When the residual RMS becomes dominated by the structured signal the ratio should start to converge. It is shown that a little less than 30 dB of RFI power reduction has been achieved, and that the reduction has not reached it limit after 2.23 seconds.*

3.3 Iridium Telecommunication Low Earth Orbit (LEO) Satellites

In this section results from an observation of an IRIDIUM satellite are presented. The observation consisted of recording 2.23 seconds of dual polarised voltage data, with 8 bit sampling at a rate of 30 MSamples per second. Data was taken while pointing toward the satellite Iridium 64. Iridium 64 has a downlink between 1616.00 - 1626.50 MHz. Iridium transmits voice and data at up to 4.8 kbits per second. Iridium uses both time and frequency multiple access methods, with up to 240 separate frequency channels. This means that the power is quickly moving around the band, which can seriously effect the optimal complex weights used in the RFI modeling. Iridium also orbit approximately seven times faster than GLONASS and GPS, meaning that many of the stationarity limitations will be occurring on a much faster time scale. This high orbital velocity also means that decorrelation of baseline power spectra due to fringe-rotation is a serious concern. While the investigation of low Earth orbit satellite RFI mitigation is only just beginning, the above analyses were applied to the IRIDIUM data for comparison. In this report each sub-correlation block is made up of 64 consecutive 1024pt-FFTs, and only the first 256 blocks have been used for the final power spectra. This is approximately 0.56 seconds of data. The observation was run on June 19, 2001, and was centred at 1621 MHz. All antennas were pointing toward the satellite with an azimuth of 58° and an elevation of 38°. Figure 13 shows the power spectra in antennas 1, 2, and 3. In all of the following plots, only the peak at 8.7 MHz will be shown, since the peaks are very narrow. The peak at 10 MHz is a system birdie, not an IRIDIUM transmission.

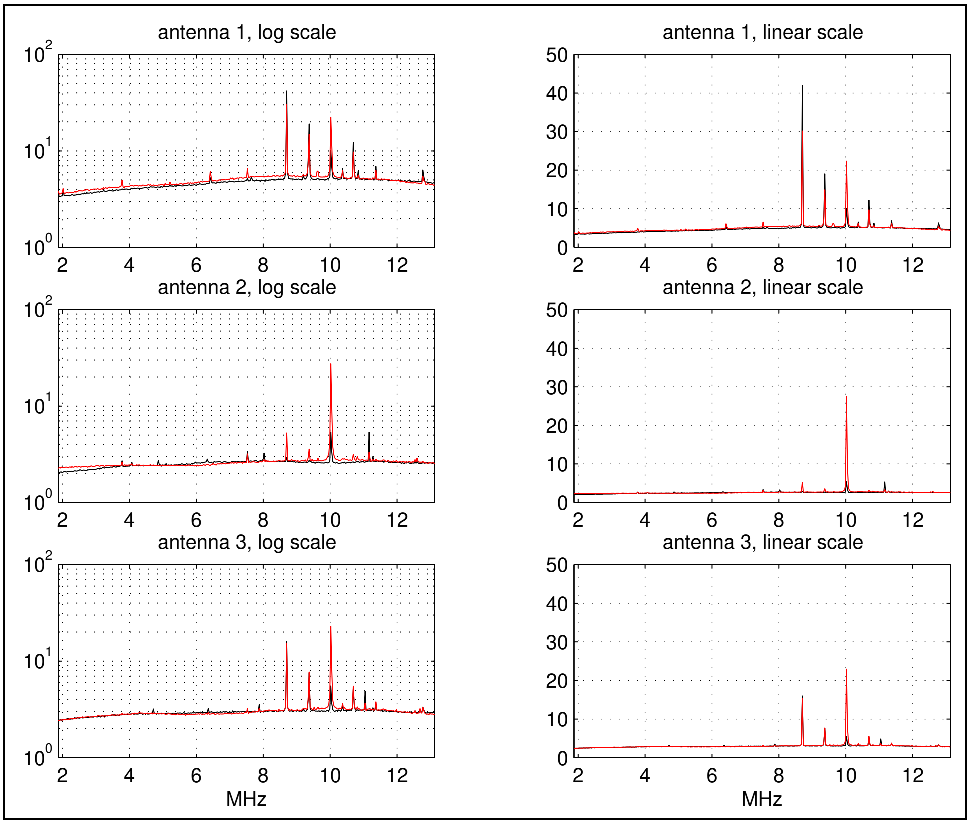

Figure 13: *Observed power in antennas 1, 2, and 3. All antennas were pointing towards IRIDIUM 64. The power was estimated by correlating the output of 64 1024-pt FFTs (2.18 ms) and averaging the results over 0.56 seconds. Red and black lines distinguish receiver polarisations. The left and right columns are equivalent, apart from log and linear vertical scales.*

Figure 14 shows the mitigation results for antennas 2 and 3, concentrating on the peak at 8.7 MHz. The voltage-domain technique does considerably worse here compared to the power-domain techniques. The most likely cause is that the weights were determined from the previous sub-correlation block, and things are changing much faster here. As mentioned above the ATA is likely to have a built-in delay to ensure that the weighting coefficients are determined by the voltage samples that they are applied to. This delay needs to be included into these algorithms.

Figure 15 shows a zoomed view of the residuals. The performance of the power domain cancellation techniques are very similar. The main reason for this is the large INR of the reference, as shown in figure 13 (note that the INR of interest is that of the 8.7 MHz peak only). Again, test should be carried out to see if the large residuals associated with voltage domain cancellation are due to using old weights.

Figure 16 shows the ratio of the RMS in the residual to raw power across the 8.7 MHz peak. Note that in this figure the x axis has a linear scale. The steps that occur every few hundred milliseconds are due to variations in the amplitude of the 8.7 MHz peak power. Antenna 3, which has a large INR reaches an RFI reduction of about 20 dB.

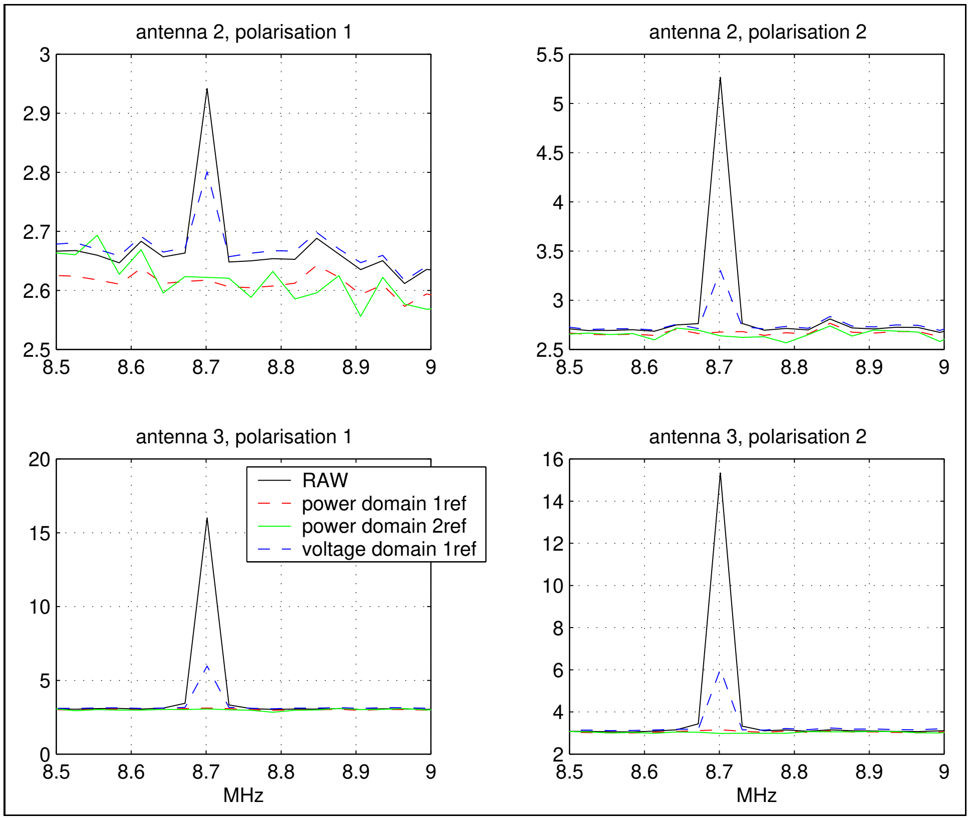

Figure 14: *Mitigation results for antennas 2 and 3, concentrating on the peak at 8.7 MHz. The voltage-domain technique performs poorly compared with the power-domain techniques. The most likely cause is that the weights were determined from the previous sub-correlation block, and things are changing much faster.*

3.4 Effect on Astronomical Signals

To investigate the effect on an astronomy signal, a synthetic 0.5 MHz wide signal was introduced into the voltage streams of the astronomy antennas with zero delay at 6 MHz. Figures 17 and 18 show the power spectra and residual power spectra from this experiment. Although a quantitative analysis is yet to be carried out, the results indicate that the algorithms have had little affect of the signal. Since the exact characteristics of this signal can be calculated, it will form the basis for a quantitative analysis.

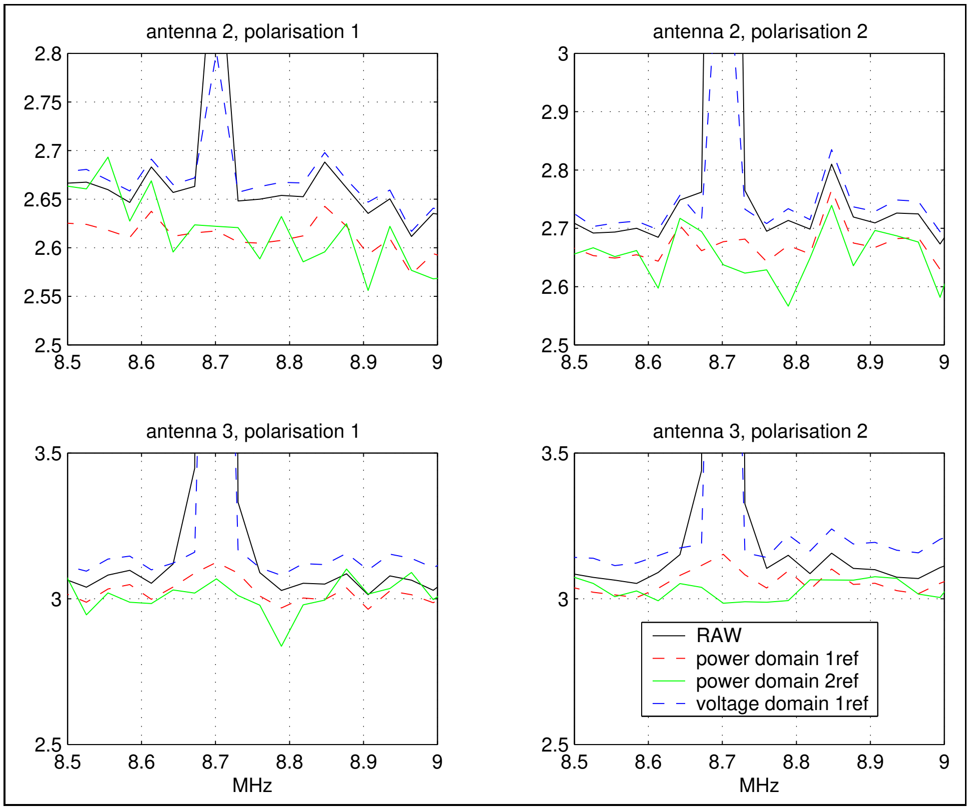

Figure 15: *Mitigation results for antennas 2 and 3, concentrating on the peak at 8.7 MHz. The voltage-domain technique performs poorly compared with the power-domain techniques. The most likely cause is that the weights were determined from the previous sub-correlation block, and things are changing much faster.*

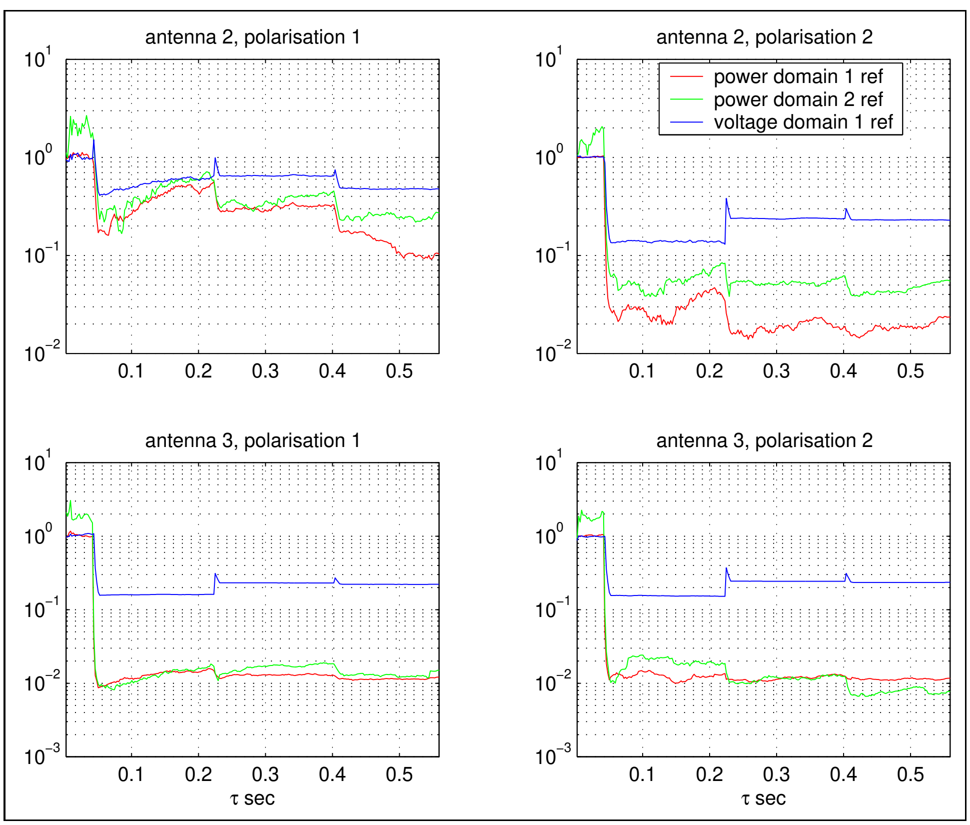

Figure 16: *RMS in the residual power divided by the RMS in the raw power over the 8.7 MHz peak. Most of the variation is due to variation in the raw amplitude of the peak.*

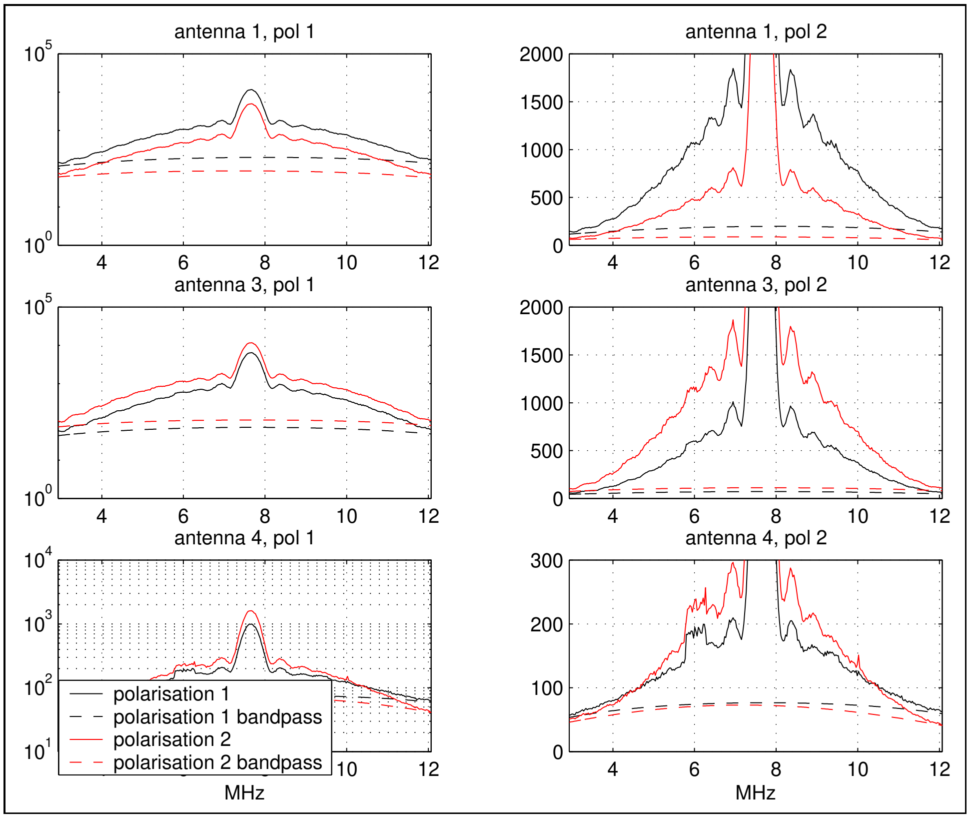

Figure 17: *Power spectra for antennas 1, 3, and 4 containing GLONASS 772 transmission. Antennas 3 and 4 have an additional synthetic 0.5 MHz signal centred at 6 MHz present. The 100% polarised synthetic signal was injected into the voltage streams of antennas 3 and 4 prior to processing.*

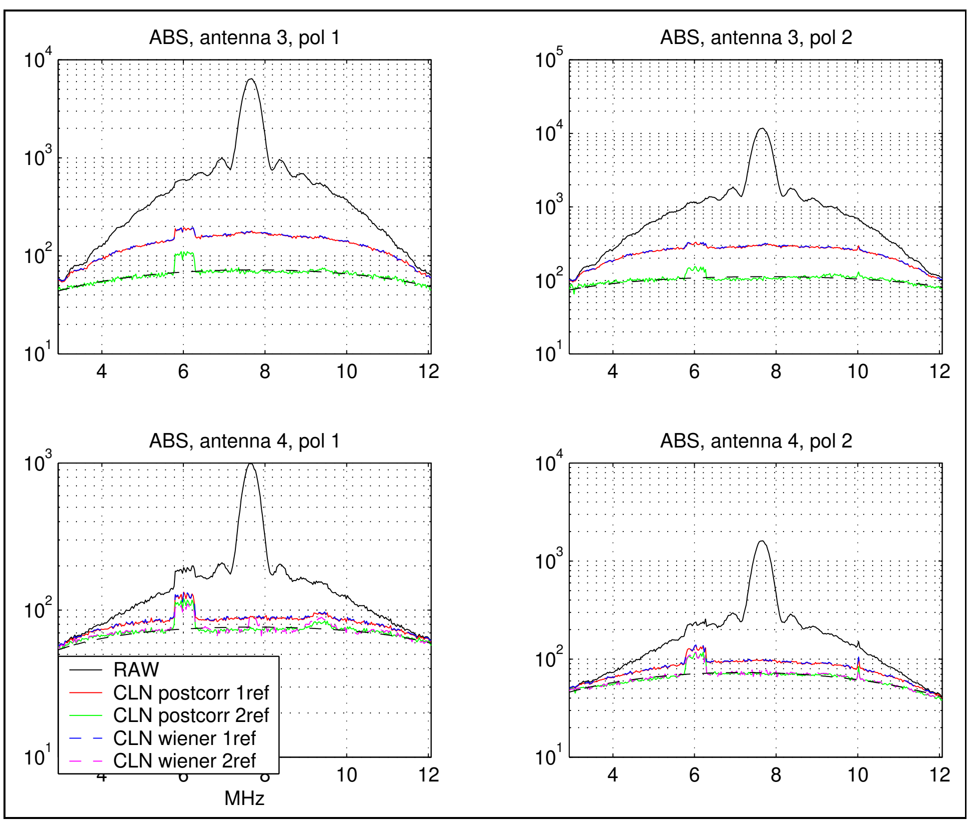

Figure 18: *Residual power for antennas 3, and 4 containing GLONASS 772 transmission plus a synthetic 0.5 MHz signal centred at 6 MHz. The 100% polarised synthetic signal was injected into the voltage streams of antennas 3 and 4 prior to processing.*

4 Summary

It has been shown quantitatively that if the optimal complex weights, given by the Wiener solution, for modeling RFI in a voltage stream using a reference voltage are stationary, then the cancellation can be made after correlation in the power domain. Cancellation in either the voltage or power domains lead to similar results. The main limitation of both methods is that the system noise of the reference voltage leads to an attenuation of the interference estimate. Using two reference signals with uncorrelated noise greatly improves the result, especially in the case of a low reference signal interference-to-noise ratio. At least 36 dB of RFI power reduction was achieved, this number limited mainly by the amount of available data.

For GLONASS and GPS interference, it has been shown that the complex weights are stable for several hundred ms (for a 10 m baseline). It is believed that this is limited mainly by the motion of the satellites, which orbit at approximately twice the sidereal rate, rather than changes in the satellite transmission. IRIDIUM satellites which orbit about seven times faster and have very complicated spectra are much harder to analyse, however almost 20 dB of RFI reduction was achieved. Much more work is needed in pin pointing the exact processes that are causing changes in the complex weights, and to what level each process is affecting the mitigation quality.

Little has been said about the effect of the techniques on astronomical signals. This is an extremely important parameter in any RFI mitigation algorithm and should be included in any detailed experiment. Data containing GLONASS signals together with OH maser emission have been taken with the RPA, and synthetic signals have also been included into the primary antenna voltage signals. While the techniques seem to leave the astronomy signals alone in the most part, the subtle effects may be extremely important and need to be known with extreme accuracy.

5 Appendices

5.1 Pre-Correlation in Time Domain (FIR Filter with Wiener Solution)

All of the voltage-domain results shown in this report were processed in the time domain rather than the frequency-domain. This involves using the reference-primary signal cross-correlation lag spectrum and the reference signal auto-correlation lag spectrum to create the optimal weights for the interference model. In the above analysis, the lag spectra were calculated by inverse Fourier transforming the power spectra.

Create a 2P-1 tap FIR filter. The idea is to find a set of 2P-1 weights w which minimise the power in $r_{A_k}(t) = v_{A_k}(t) - m_{A_k}(t)$, where $m_{A_k}(t)$ is a model of the RFI voltage in $v_{A_k}(t)$, based on the reference voltage,

$$m_{A_k}(t) = \sum_{k=1-P}^{P-1} w_{A_k,k}(t) v_{R_x}(t-k).$$

Similarly to the frequency domain version, the weights are given by

$$w_{A_k}(t) = \mathbf{C}_{R_x,R_x}^{-1} C_{A_k,R_x}$$

where the bold faced $\mathbf{C}_{R_x,R_x}$ indicates a (2P-1)*(2P-1) matrix formed from the lag spectra of the reference signal. This can be written out as the individual lags

$$w_{A_k}(t) = \begin{bmatrix} C_{R_x,R_x}(0) & C_{R_x,R_x}(1) & \cdots & C_{R_x,R_x}(2P-2) \\ C_{R_x,R_x}(1) & C_{R_x,R_x}(0) & \cdots & C_{R_x,R_x}(2P-3) \\ \vdots & \vdots & \ddots & \vdots \\ C_{R_x,R_x}(2P-2) & C_{R_x,R_x}(2P-3) & \cdots & C_{R_x,R_x}(0) \end{bmatrix}^{-1} \begin{bmatrix} C_{A_k,R_x}(1-P) \\ \vdots \\ C_{A_k,R_x}(1) \\ C_{A_k,R_x}(0) \\ C_{A_k,R_x}(1) \\ \vdots \\ C_{A_k,R_x}(P-1) \end{bmatrix}$$

The model is then found by summing together 2P-1 laged versions of the reference signal, weighted by the w_{A_k} terms

$$m_{A_k}(t) = \begin{bmatrix} v_{R_x}(P-1) & \cdots & v_{R_x}(0) & \cdots & v_{R_x}(1-P) \\ v_{R_x}(P) & \cdots & v_{R_x}(1) & \cdots & v_{R_x}(2-P) \\ v_{R_x}(P+1) & \cdots & v_{R_x}(2) & \cdots & v_{R_x}(3-P) \\ \vdots & \cdots & \vdots & \cdots & \vdots \\ v_{R_x}(N+P-2) & \cdots & v_{R_x}(N-1) & \cdots & v_{R_x}(N-P) \end{bmatrix} \begin{bmatrix} w_{A_k,1-P} \\ \vdots \\ w_{A_k,-1} \\ w_{A_k,0} \\ w_{A_k,1} \\ \vdots \\ w_{A_k,P-1} \end{bmatrix}$$

This was the method used to generates the voltage-domain results. The notation differs from most reports, since here the negative time lags have been included. See [2] for a detailed description of the technique.

References

[1] R. D. Ekers & J. F. Bell. "Radio Frequency Interference". In *The Universe at Low Radio Frequencies,*. IAU Symposium, December 1999.

[2] G. C. Bower. "Application of Wiener and Adaptive Filters to GPS and Glonass Data from the Rapid Prototyping Array". ATA Memo 31., August 2001.

[3] C. Barbaum & R. Bradley. "A new approach to interference excision in radio astronomy: real-time adaptive cancellation". *Astronomical Journal*, page 116, 1998.

[4] S. Haykin. *Adaptive Filter Theory*. Prentice Hall.

[5] F. H. Briggs & J. F. Bell & M. J. Kesteven. "Removing Radio Interference from Contaminated Astronomical Spectra Using an Independent Reference Signal and Closure Relations". *AJ*, December 2000.

[6] B. Widrow & S. Stearns. *Adaptive Signal Processing*. Prentice Hall.